

A Method for Predicting Flux Loss of Multi-pole Magnet and Its Evaluation

Hirotohi Fukunaga¹, Shohei Narikiyo¹, Hiroyuki Koreeda¹, Takeshi Yanai¹, Masaki Nakano¹,
and Fumitoshi Yamashita²

¹Graduate School of Engineering, Nagasaki University, Nagasaki 852-8521 Japan

²Rotary Component Technology Development Division, Minebea Co., Ltd., Shizuoka 437-1193

The prediction of flux loss due to exposure at an elevated temperature is very important in applications of Nd-Fe-B magnets because of the low Curie temperature of the Nd₂Fe₁₄B. Previously, we proposed the prediction method of the initial flux loss, FL_{int} , from basic magnetic properties of a magnet by taking advantage of the finite element method. The prediction method takes the magnetizing process and the distribution of coercivity into account, and is composed of four steps, (i) simulation of distribution of magnetization under magnetizing field, (ii) determination of demagnetization curves at room and exposure temperatures, (iii) simulation of distributions of magnetization at room and exposure temperatures, and finally (iv) prediction of distribution of FL_{int} . We applied this method to a Nd-Fe-B ring magnet with 12 poles, and predicted FL_{int} due to the exposure at 120 °C. Subsequently, the prediction method was evaluated by comparing the predicted FL_{int} values with the experimental ones. The predicted FL_{int} values agreed with those obtained experimentally, which suggests the validity of the proposed method.

Index Terms—Coercivity, flux loss, magnetization process, Nd-Fe-B magnet, permanent magnet motor.

I. INTRODUCTION

Nd-Fe-B magnets have been applied to electrical and electronic devices such as motors. In some applications of magnets, the magnets are exposed at an elevated temperature, which causes an irreversible reduction in flux. This reduction in flux is not recovered even if the magnets are cooled to room temperature, and is called “flux loss”. The flux loss is categorized into three types, the permanent, initial, and long-term ones [1]. Generally, the initial flux loss FL_{int} , which originates from decrease in coercivity at an exposure temperature, is particularly important, because it is a large reduction in flux in a short time. As the Curie temperature of Nd₂Fe₁₄B [2] is much lower than those of SmCo₅ and Sm₂Co₁₇ [3], Nd-Fe-B magnets have a tendency of exhibiting a large FL_{int} value.

In many applications of a magnet, the magnet is magnetized multi-porlarly, and FL_{int} depends on local demagnetizing field in the magnet. Furthermore, FL_{int} is affected in the magnetized state of the magnet, because the coercivity of the magnet depends on magnetizing field experienced. Thus, methods of predicting FL_{int} of a magnet with complicated shape were proposed by some researchers [4, 5]. Those methods, however, cannot take the distribution of coercivity into account and the pre-measurement of FL_{int} are necessary for magnets with various permeance values.

In order to avoid the above difficulties, we have proposed a method of predicting FL_{int} from basic magnetic properties under consideration of the distribution of coercivity [6]. In this contribution, we improved the method proposed previously, applied it to a Nd-Fe-B ring magnet with 12 poles, and predicted FL_{int} due to an exposure at 120 °C. Subsequently, the prediction method was evaluated by

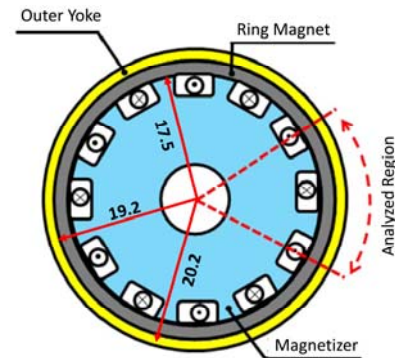


Fig.1 Ring magnet assumed in this investigation. The magnetizer is also shown with its conductors. The prediction of the initial flux loss was carried out for the one sixth part of the whole magnet shown by the broken arrow.

comparing the predicted FL_{int} values with the experimental ones.

II. PREDICTION PROCEDURE OF INITIAL FLUX LOSS

A. Model

Figure 1 shows the model of the ring magnet used for the prediction of FL_{int} together with the magnetizer. The isotropic resin-bonded Nd-Fe-B magnet was assumed and its outer and inner diameters were set at 38.4 and 35.0 mm, respectively. The magnet was magnetized at room temperature, which is set at 25 °C in this investigation, so as to have 12 poles with a magnetizer by the pulse current of 22 kA. After the magnetization, it was removed from the magnetizer and was exposed at 120 °C. We define FL_{int} inside and outside of the magnet as

$$FL_{int} = (I_0 - I_1)/I_0, \quad (1)$$

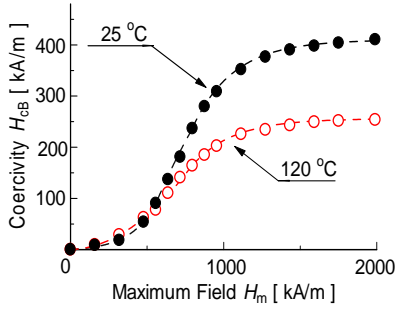


Fig.2 Measured and approximated coercivity H_{cB} as a function of maximum magnetic field which the magnet experienced.

$$FL_{int} = (B_0 - B_1)/B_0, \quad (2)$$

where I_0 and B_0 are the magnetization and the flux density before the exposure, respectively, and I_1 and B_1 are those measured at room temperature after the exposure.

The prediction of FL_{int} was carried out for the one sixth part of the whole magnet shown in Fig.1 by the broken arrow.

B. Measurement and Approximation of Basic Magnetic Properties

Magnetization and demagnetization curves were measured with a vibrating sample magnetometer for cubic samples, 3 mm in size. Samples were magnetized under a certain maximum applied field at room temperature. Then, the demagnetization curves at 25 °C or 120 °C were measured for each sample. The experienced maximum magnetic field H_m of the samples was varied from 0.14 to 2 MA/m.

The measured coercivity H_{cB} was approximated with analytical function of H_m . The flux density B in the second quadrant was approximated with parabolic function of the effective applied field H as

$$B(H) = a_1(H - H_{cB}) + a_2(H - H_{cB})^2 \quad (3)$$

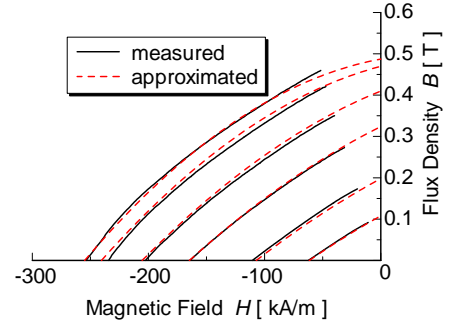
where a_1 and a_2 are the coefficients of 1st and 2nd order terms, respectively. The values of a_1 and a_2 were determined as an analytical function of H_{cB} by the least-squares method. As H_{cB} is approximated as a function of H_m , we can deduce a_1 and a_2 and resultantly demagnetization curves from H_m . This procedure enables us to deduce the B vs. H curves for any value of H_m . The measured and approximated coercivity H_{cB} and demagnetization curves are shown in Figs.2 and 3, respectively. It is seen that H_{cB} and the demagnetization curves are well fitted by the method explained above.

C. Prediction of FL_{int}

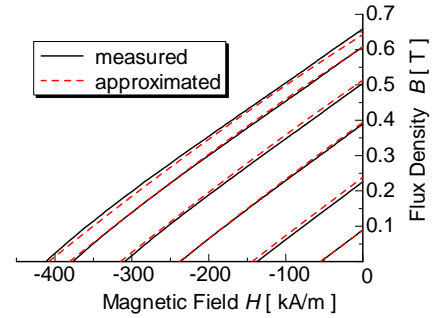
The FL_{int} value in a magnet can be calculated from

$$(FL)_{int-cal} = \frac{1 - I_w(T_{ex})}{I_w(T_{rt}) \{1 - \alpha(T_{ex} - T_{rt})\}} \quad (4)$$

where $I_w(T_{rt})$ and $I_w(T_{ex})$ are the magnetization values of at



(a) 120 °C



(b) 25 °C

Fig.3 Measured and approximated demagnetization curves for the bonded magnet used in this investigation at (a) 120 °C and (b) 25 °C. The experienced maximum fields were 0.48, 0.64, 0.8, 0.96, 1.28, and 2 MA/m.

room temperature T_{rt} and the exposure temperature T_{ex} , respectively, and α is the temperature coefficient of the remanence. The physical meaning of (4) and its validity have been reported elsewhere [7,8].

We predicted FL_{int} by using a commercially available two-dimensional FEM (Finite Element Method) program and (4). Our prediction method takes the magnetizing process and the distribution of coercivity into account, and is composed of four steps, (i) simulation of distributions of magnetization under magnetizing field by FEM, (ii) determinations of coercivity H_{cB} and demagnetization curves at room and exposure temperatures by the procedure indicated in Section B, (iii) simulation of distributions of magnetization at room and exposure temperatures by FEM, and finally (iv) prediction of the distribution of FL_{int} by usage of (4). The detailed procedure of our prediction method has been reported elsewhere [6].

In Step (ii), we determined the H_{cB} value from the magnitude of H_m , although H_{cB} had been determined from the radial component of H_m in the previous report [6]. Subsequently, we defined H_{cB} values for radial and circumference directions. This treatment of H_{cB} improved the accuracy of the simulation significantly.

D. Measurement of FL_{int}

The ring magnet was prepared from isotropic Nd-Fe-B powder. Its outer and inner diameters and the height are 38.4, 35.0, and 4.0 mm, respectively. The diameters are the same

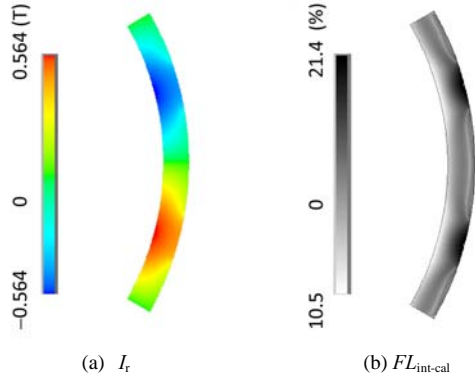


Fig.4 Distributions of (a) the radial component of magnetization I_r before exposure and (b) the predicted flux loss of I_r , $FL_{int-cal}$, due to the exposure at 120 °C. The result for one sixth of the whole magnet is shown.

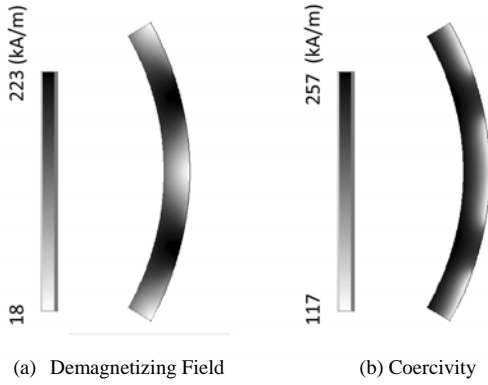


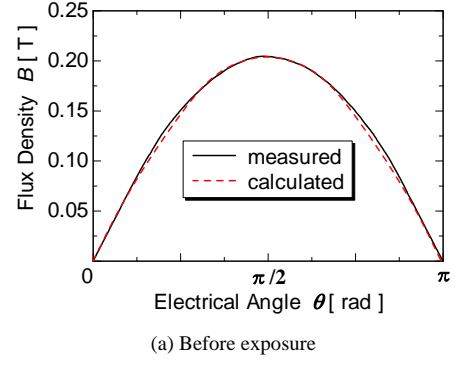
Fig.5 Distributions of magnitude of (a) demagnetizing field and (b) coercivity in the ring magnet at 120 °C. The results for one sixth part of the whole magnet are shown.

with those shown in Fig.1. The prepared magnet was magnetized at 25 °C, and exposed at 120 °C for 1 h according to the procedure indicated in Section A. We measured the distributions of the perpendicular component of the flux density on the inner surface of the ring magnet with a magnet analyzer (IMS Co. Ltd., MTX-103L) before and after exposure at 25 °C. The initial flux loss FL_{int-ex} was deduced from (2).

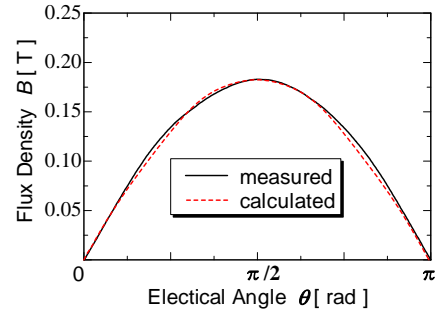
III. RESULTS OF PREDICTION OF FL_{int}

Figure 4 show the distributions of (a) the radial component of magnetization I_r before the exposure and (b) the predicted flux loss of I_r , $FL_{int-cal}$, due to the exposure at 120 °C. It is seen that large flux loss is expected at the centers of magnetic pole near the outer surface of the magnet. It is also found that FL_{in} is small in the vicinity of the inner surface. The $L_{int-cal}$ value averaged over the whole magnet is 15.5 %.

In order to clarify the origins of the large flux loss near the outer surface, the distributions of the demagnetizing field and H_{cB} at 120 °C were calculated, and the results are shown in Fig.5. The demagnetizing field is large at the centers of magnetic poles near the outer surface. These large demagnetizing fields would be responsible for the large flux



(a) Before exposure



(b) After exposure

Fig.6 Flux densities of inner surface of the ring magnet (a) before and (b) after exposure as a function of electrical angle θ . The predicted and measured results are shown by solid and broken lines, respectively. The measurements were carried out at 25 °C.

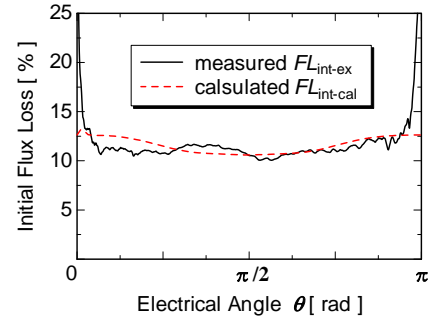


Fig.7 Predicted and measured initial flux losses as a function of electrical angle θ .

loss values in this region. On the other hand, H_{cB} is large in the vicinity of the inner surface. Therefore, small $FL_{int-cal}$ values in the vicinity of the inner surface can be attributed to large H_{cB} values in this region.

IV. COMPARISON OF $FL_{int-cal}$ WITH FL_{int-ex}

The flux density on the inner surface was measured at 25 °C before and after exposure, and FL_{int-ex} was calculated from (2). Subsequently, the results were compared with predicted one. The results are shown as a function of electrical angle in Fig.6. The predicted flux densities before and after the exposure agree well with the measured ones. The measured flux loss, FL_{int-ex} , also agrees with the predicted one, $FL_{int-cal}$, except the vicinities of the electrical angles of 0 and π as seen in Fig.7,

where $FL_{\text{int-ex}}$ has a tendency to diverse. Small flux density in these regions is responsible for this divergence of $FL_{\text{int-ex}}$ as understood from (2). The averages of $FL_{\text{int-cal}}$ and $F_{L_{\text{int-ex}}}$ are 11.6 and 11.9 %, respectively, and they agree with each other. Consequently, these results strongly suggest that the proposed method is useful in the prediction of the initial flux loss of multi-polarly magnetized magnets.

V. CONCLUSIONS

The initial flux loss due to the exposure at 120 °C was predicted for a Nd-Fe-B ring magnet with 12 poles from basic magnetic properties under consideration of the magnetization process and the distribution of coercivity of the ring magnet. The proposed method enabled us to simulate the distributions of magnetization in the magnet before and after the exposure at an elevated temperature, and consequently the initial flux loss.

In order to evaluate the validity of the proposed method, the ring magnet was prepared and exposed according to the same procedure with the prediction. The distributions of the flux densities before and after the exposure on the inner surface of the magnet were measured, and the initial flux loss was deduced for the prepared magnet. The results obtained experimentally were compared with those predicted, and it was found that the experimental and predicted results agree with each other. These results strongly suggest that the proposed method is useful in the prediction of the initial flux loss of multi-polarly magnetized magnets.

REFERENCES

- [1] A.G. Clegg, I.M. Coulson, G. Hilton, and H.Y. Wong, "The Temperature Stability of NdFeB and NdFeBCo Magnets," *IEEE Trans. Magn.* vol. 26, pp.1942–1944, Sep. 1990.
- [2] M. Sagawa, S. Fujimura, H. Yamamoto, Y. Matsuura, and K. Hiraga, "Permanent magnet materials based on the rare earth-iron-boron tetragonal compounds," *IEEE Trans. Magn.* vol.20, pp.1584–1589, Sep. 1984.
- [3] K.H.J. Buschow, "Rare Earth Compounds" in *Ferromagnetic Materials* vol. 1, E.P Wohlfarth, Ed. Amsterdam: North-Holland, 1988, pp. 365–369.
- [4] K. Itoh, Y. Hashiba, K. Sakai, and T. Yagisawa, "The flux condition of the magnetic circuit with a permanent magnet taking into account the long-time stability," *Trans. IEE Jpn.* vol. 118-A, pp.176–181, Feb. 1998 (in Japanese).
- [5] K. Miyata "High-precision Modeling for Magnetic Field Analysis of Permanent Magnet Motor – Considering Alignment, Magnetizing and Demagnetizing –," *National Conv. Record IEE Jpn.* 5-S16-4, pp. 2157–2160, Mar. 2001 (in Japanese).
- [6] H. Fukunaga, H. Koreeda, T. Yanai, M. Nakano, and F. Yamashita, "Prediction of flux loss in a Nd-Fe-B ring magnet considering magnetizing process," *J. Phys.: Conf. Ser.* vol. 200, pp.082006–1–4, Mar. 2010.
- [7] Y. Kanai, S. Hayashida, H. Fukunaga, and F. Yamashita, "Flux Loss in Nanocomposite Magnets," *IEEE Trans. Magn.* vol. 35, pp.3292–3294, Sep. 1999.
- [8] H. Fukunaga, R. Yamamoto, and F. Yamashita, "Highly Stable Nd-Fe-B Bonded-Magnets Using Spherical Powder Prepared by Spinning-Cup Atomization," in *Proc. 18th Int. Workshop on High Performance Magnets and Their Applications*, N.M. Dempsey and P. de Rango Eds. Annecy:2004, pp.229–235.